Published in final edited form as:
J Phys Chem C Nanomater Interfaces. 2007 ; 111(19): 7091–7097. doi:10.1021/jp067635q.

Sulforhodamine Adsorbed Langmuir-Blodgett Layers on Silver Island Films: Effect of Probe Distance on the Metal-Enhanced Fluorescence

Krishanu Ray, **Ramachandram Badugu**, and **Joseph R. Lakowicz***
Center for Fluorescence Spectroscopy, University of Maryland School of Medicine, Department of Biochemistry and Molecular Biology, 725 West Lombard Street, Baltimore, MD 21201, USA

Abstract

Metal-Enhanced Fluorescence (MEF) has become an important method in biomedical sensing. In this paper, we present the distance-dependent MEF of sulforhodamine B (SRB) monolayer on silver island films (SIFs). SRB is electrostatically incorporated into the Langmuir-Blodgett (LB) layers of octadecylamine (ODA) deposited on glass and SIFs substrates. The distances between SRB and SIFs or glass surfaces are controlled by depositing a varied number of inert stearic acid (SA) spacer layers. SRB is incorporated into positively charged LB layers of ODA by immersing the ODA deposited substrates into aqueous solution of SRB. Dye incorporated ODA layers with 10 nm separation distance from the SIFs surface show maximum metal-enhanced fluorescence intensity; ~7-fold increase in intensity as compared to that from the glass surface. The corresponding enhancement factor is reduced with increasing or decreasing the probe distance from the SIFs surface. Additionally, SRB on SIF surfaces show reduced lifetimes. We observed the shortest lifetime from the SRB with 5 nm distance from the SIF surfaces and the lifetime increased consistently with increasing the distances between the fluorophore and the SIFs surface. These observed spectral changes, increase in fluorescence intensity and decreased fluorescence lifetimes, are in accordance with the expected effects due to near-field interactions between the silver nanoparticles and fluorophores. We have also analyzed the complex fluorescence heterogeneous decays on metallic nanostructured surfaces using continuous distributions of decay times. The decay-time distributions appear to be sensitive to the distance between the metal and fluorophore and represent the underlying heterogeneity of the samples. The present systematic study provides significant information on the effect of fluorophore distance on the metal-enhanced fluorescence phenomenon.

1. Introduction

In recent years there have been many investigations of the optical properties of molecules in the proximity of metallic nanoparticles or rough surfaces.[1–9] Metallic structures can have a number of effects on the spectral properties of nearby fluorophores. Metals are traditionally considered as a quencher for radiating emitters specifically in the near-field regime. However, the luminescence and Raman signals can be enhanced on metallic nanostructures. Metallic interfaces display complex interactions of the local electromagnetic fields with fluorophores. A metallic particle near a fluorophore can influence both its excitation and emission, eventually leading to significantly enhanced spectral properties. The metal-enhanced fluorescence (MEF)[10–13] effect can yield an increase in the quantum yield, and reduction in fluorescence lifetime of emitting fluorophores that are held in close proximity to noble metal surfaces that are roughened on the nanometre scale. The MEF effect derives from the interaction of the dipole

E-Mail: Lakowicz@cfs.umbi.umd.edu.

moment of the fluorophore and the surface plasmon field of the metal resulting in an increase in the radiative decay rate and stronger fluorescence emission. Fluorescence lifetimes of molecules near metal surfaces are dramatically affected by the electromagnetic interaction between the excited molecules and the metal surface. MEF is also described as radiative decay engineering (RDE) since the radiative decay rate of fluorophores can be controlled by the careful engineering of the chemical environment and physical morphology of the nanopatterned metal surfaces.[3,10] A critical MEF parameter is controlling the precise distance (5–20 nm) at which the fluorophores are located from the metal surface to render maximum fluorescence intensity.[14–17] In some cases, a dielectric (such as silica) coating of required thickness can be evaporated over the SIF, or a molecular spacer that binds directly to metal surfaces (e.g. thiols with silver/gold) of the desired length can be used. In none of these cases the probe distance and orientation was well controlled. The study of MEF and its applications is still in its infancy and there is a need to develop further understanding of the fundamental physics and chemical processes that govern MEF before practical applications can be developed. The controlled construction of ordered molecular structures on metallic nanostructures will help in understanding the meal-fluorophore interaction in greater detail. Although the distance between the probe and metallic surface is precisely controlled, the variations in molecular orientations might lead to the varied enhancement factor.[18,19]

Langmuir-Blodgett (LB)[20] films provide controlled distance and well-defined orientation of fluorophores on metallic nanostructures. The structure, composition and thickness of the LB films can be precisely controlled at the molecular level. The fluorophores deposited by the LB technique are expected to be at one distance rather than a range of distances from the metal surface or the metal island films, but of course there will still be in-plane heterogeneity of fluorophores on or between the metal particles. Additionally, the probe orientation with surface normal is fixed and maintained in every LB monolayer irrespective of the distance from the surface. Not all fluorescence probes are suitable for orientation in LB films. Typically the probes should consist of at least one long alkyl-chain (tail) and a hydrophilic head group. In order to better understand the distance effect on MEF, it is advisable to study the distance dependence behavior of several different probes. Accordingly, we combined the LB technique that provides useful precisely controlled layers with electrostatic adsorption technique. Using adsorption technique, the anionic probes such as sulforhodamine B (SRB) can be electrostatically incorporated into cationic octadecylamine (ODA) layers, as in the present case, and cationic probes can be incorporated into anionic LB layers deposited on surfaces that can be used for MEF. Combination of these two techniques offer well-controlled distance and orientation for a wide variety of probes including amphiphilic, nonamphiphilic and water-soluble ionic dyes from the surface.[21]

In this paper, we present how the fluorescence intensity and radiative decay rates of sulforhodamine B (SRB) molecules are affected as a function of distance between the fluorophore and silver island films (SIFs). The incorporation of sulforhodamine B (SRB) in the octadecylamine LB films was reported previously.[21] The adsorption process mainly occurred due to the ionic interaction between the cationic amino group of the long-chain amine and the sulfonic group of the SRB dye. The orientation of the SRB dye molecule in the LB films determined by polarized absorption spectra indicated a lying-flat orientation of the SRB molecule. Structural characteristics of the SRB adsorbed octadecylamine LB films such as orientation, layer-layer distance, and topography of the film surface were studied by FTIR spectroscopy, low-angle X-ray diffraction, and atomic force microscopy (AFM).[21] The separating distances between the SIFs surface and fluorophore are controlled by varying the numbers of inert stearic acid LB layers. Hence this system of SRB in LB films provides an ideal opportunity to study the distance dependence of MEF using several commonly available probes.

2. Experimental details

Sulforhodamine B (SRB), Stearic acid (SA), octadecylamine (ODA), (Figure 1) spectroscopic grade chloroform were obtained from Aldrich and used without further purification. Deionized water, purified using Millipore Milli-Q Gradient System, was used for LB monolayer deposition and in all other chemical modifications. Silver nitrate, ammonium hydroxide, sodium hydroxide, glucose were purchased from Aldrich and used as received. Silver island films were deposited on clean glass slides (Corning, NY) using the method reported previously by us.[15] The SIFs slides were stored in Milli-Q water until they were used for LB deposition. SIFs coated on glass slide displayed the characteristic surface plasmon resonance with an absorption maximum near 460 nm.

LB film depositions on glass and SIFs coated glass are accomplished using computer controlled KSV 5000 LB trough. Milli-Q deionized water (at 20 °C, with resistivity of 18.2 M -cm) was used as water subphase. The pH of water used was 5.8 and 10.3 for the deposition of steric acid and octdecylamine LB layers, respectively. The pH of the subphase was adjusted with NaOH or HCl. The pure stearic acid or octadecylamine monolayers on the water subphase were formed by spreading a known concentration of stearic acid or octadecylamine in chloroform. After allowing for 15 minutes to evaporate the solvent chloroform, the monolayer at the air-water interface was slowly compressed to an optimum surface pressure (20 and 45 mN/m for SA and ODA monolayer, respectively). Subsequently, the compressed monolayer was transferred by the LB technique onto the solid substrates, where a clean glass and a SIFs coated glass slides were sandwiched together and monolayers were deposited at a dipping speed of 7 mm/min. The initial layer on the surface was obtained during the upstroke giving rise the head group of the amphiphilic SA or ODA deposited in contact with the surface of the substrate. The observed monolayer transfer ratio from the compressed water subphase to substrate was ~0.95. A schematic representation of LB layers with varied distance between the ODA layer and SIFs surface is shown in Figure 2. We first deposited a monolayer of ODA directly onto both glass and SIFs surfaces to obtain the probe layer with 0 nm distance from the surfaces. Subsequently, to get the probe layer with defined distance from the surfaces we deposited the required number (*i.e.* 1, 3, 5, 9 or 19) of steraic acid layers followed by two ODA layers (Figure 2). Each stearic acid layer on the surface provides 2.5 nm distance. Subsequently, by using 1, 3, 5, 9 and 19 layers of stearic acid results the probe layers on glass and SIFs surfaces with distances (d) of 5, 10, 15, 25 and 50 nm, respectively. After the layers were completely dried at ambient conditions, SRB was incorporated into the ODA layers by immersing in aqueous SRB solution for about 5 min. To avoid any probe aggregation in ODA layers we used lowest possible concentration of 1×10^{-6} M and short period of immersing time (5 min). It is important to note here that SRB molecules could not be incorporated into the LB films of only stearic acid with any number of layers, indicating the electrostatic interactions between negatively charged SRB and positively charged ODA are necessary for probe incorporation into the films. The SRB adsorbed LB film on glass shows characteristic absorption and fluorescence spectra that can be ascribed to be originated from the monomeric SRB dye incorporated into the ODA layers. The observed absorption and fluorescence band maximums were 565 and 585 nm, respectively. Polarized absorption spectroscopic study reveals the SRB transition dipole moment orientation in the ODA LB layers is 73° which is in agreement with our previous report.[21]

Absorption spectra were collected using a Hewlett-Packard 8453 spectrophotometer. Fluorescence spectra of monolayers on solid substrates were recorded using a Varian Cary Eclipse Fluorescence Spectrophotometer using front face illumination geometry with 514 nm excitation from a Xenon arc lamp. Time-resolved intensity decays were recorded using a PicoQuant Fluotime 100 time-correlated single-photon counting (TCSPC) fluorescence lifetime spectrometer. The excitation source was a pulsed laser diode (PicoQuant PDL800-B)

with a 20 MHz repetition rate. The Instrument Response Function (IRF) is about 60 ps. The excitation was vertically polarized and the emission was recorded through a polarizer oriented at 54.7° from the vertical position. A bandpass filter at 570–630 nm (Chroma Inc.) was used in the collection path, thus eliminating the scattered excitation light and collecting the fluorescence from the SRB probes in the region of interest.

The fluorescence intensity decays were analyzed in terms of the multi-exponential model[22]:

$$I(t)=\sum_{i=1}^{n}\alpha_i \exp(-t/\tau_i) \tag{1}$$

where, τ_i are the lifetimes with amplitudes α_i and $\sum_i \alpha_i = 1.0$. The contribution of each component to the steady-state intensity is given by:

$$f_i=\frac{\alpha_i \tau_i}{\sum_j \alpha_j \tau_j} \tag{2}$$

The average lifetime is represented by:

$$\bar{\tau}=\sum_i f_i \tau_i \tag{3}$$

and the amplitude-weighted lifetime is given by:

$$<\tau>=\sum_i \alpha_i \tau_i \tag{4}$$

The values of μ_i and τ_i were determined using the PicoQuant Fluofit 4.1 software with the deconvolution of instrument response function and nonlinear least squares fitting. The goodness-of-fit was determined by the χ^2 value.

The intensity decays are also analyzed in terms of a lifetime distribution. For a lifetime distribution model μ_i values are replaced by distribution functions $\mu(\tau)$. The total intensity $I(t)$ is given by

$$I(t)=\int_{\tau=0}^{\infty} \alpha(\tau) e^{-t/\tau} d\tau \tag{5}$$

where $\int \alpha(\tau) d\tau = 1$. For a bimodal distribution equation 5 is used with two terms within the integral. We assumed the distributions were Gaussian with

$$\alpha(\tau)=\frac{1}{\sigma\sqrt{2\pi}} \exp\left[-\frac{1}{2}\left(\frac{\tau-\bar{\tau}}{\sigma}\right)^2\right] \tag{6}$$

where &τmacr; is the central value of the distribution, σ is the standard deviation of the Gaussian and the FWHM is 2.345σ.

3. Results and Discussion

Figure 3A shows the fluorescence emission spectra of SRB incorporated into ODA layers with a 10 nm separation distance from the glass and SIFs surfaces. The fluorescence spectra were collected at the same excitation and detection conditions allowing a direct comparison between the two substrates. The incorporated SRB has emission band maximum of ~585 nm from both glass and SIFs surfaces. Very similar spectral features, except difference in fluorescence

intensity, from SRB incorporated into the ODA layers have been observed from the metalized and non-metalized areas (Figure 3B). Accordingly, a significant enhancement of ~7-fold in fluorescence intensity from the SRB layers on SIFs surface is noticed (Figure 3). The enhancement factor is the ratio of integrated intensities of SRB detected on SIFs and glass substrates and appears to be uniform across the 550–700 nm spectral range.

To further characterize the observed MEF, we measured the fluorescence intensity decays from the dye incorporated into LB layers on both glass and SIFs surfaces using time-correlated single photon counting (TCSPC) instrument. The corresponding intensity decays observed for the SRB on glass and SIFs with a 10 nm distance from the surfaces are shown in Figure 4. The solid-lines indicate the best fit to the experimental decay curves. As can be seen from the figure, the intensity decay of SRB dye on SIFs is faster than that on glass surface. The fluorescence lifetime of SRB incorporated in the ODA layer is significantly (~5-fold) shortened when the layer is on SIFs surface. This shortening of lifetime on SIFs strongly supports that the increase in fluorescence intensity (Figure 3) is due the interaction of SRB molecules with the silver nanoparticles.[11,15,19] Nobel metal colloids exhibit strong scattering properties[23–25] and the scattering from colloids may contribute to the observed short lifetime. We have taken sufficient precautions to make sure the observed reduced lifetime, especially the short component in the probe intensity decay from the SIFs surface is not due to the scattered light but due to the SRB emission. Control measurements on the glass or SIFs substrates, without SRB, yielded almost no signal when observed through the combination of filters used to detect the SRB emission.

The quantum yield and lifetime of a fluorophore are given by:

$$\Phi_0 = \frac{\Gamma}{\Gamma + k_{nr}} \tag{7}$$

$$\tau_0 = \frac{1}{\Gamma + k_{nr}} \tag{8}$$

where Γ is the intrinsic radiative or emissive rate and k_{nr} represents all the other rate processes returning the molecule to the ground state without emission. In presence of metal nano-particles equation 7 & 8 are modified as:

$$\Phi_m = \frac{N_r \Gamma}{N_r \Gamma + k_{nr}^{/}} \tag{9}$$

$$\tau_m = \frac{1}{N_r \Gamma + k_{nr}^{/}} \tag{10}$$

In terms of radiative decay engineering model, the radiative decay rate is increased to $N_r \Gamma$ in the presence of metallic nanostructures. k'_{nr} is nonradiative rate in the presence of metal particles.

The simultaneous increase in fluorescence intensity and decrease in lifetime indicates an increased radiative decay rate in the presence of silver particles.[3] This unusual effect is due to a change in the radiative decay rate of the fluorophores, which depends on the photonic mode density near the fluorophores[3], seems to be responsible for the observed 7-fold enhancement in fluorescence and ~5-fold decrease in fluorescence lifetime of LB monolayers on SIFs.

It is important to understand the effect of fluorophore-to-metal distance on the changes in the intensities and lifetimes of the fluorophore. Fluorescence emission spectra from SRB incorporated into the ODA layers with varied distances from the SIFs surface are shown in Figure 5. Also shown in the figure is the emission spectrum of SRB incorporated into ODA

layers on glass (dash line), whose intensities are insensitive to the distance from the glass surface. Figure 6 shows the effect of distance on the fluorescence enhancement. As seen from the figure, the highest MEF of ~7-fold is noticed for the SRB incorporated ODA layers with the probe distance of 10 nm from the SIFs surface and enhancement factor is consistently reduced with increasing the probe distance from 10 to 50 nm. The lowest MEF of about 2-fold is observed from the SRB layer deposited on SIFs with a 50 nm separation distance. This substantiates that the MEF is indeed dependent on probe distance from the metallic surface. Interestingly, we also observed the monotonic decrease in MEF (from 7.5-fold to 2.0-fold) with decreasing the probe distance from 10 to 0 nm. The reduction in enhancement factor below 10 nm might due to the known fluorescence quenching ability of the metal particles on common fluorophores. Accordingly, the observed net fluorescence enhancement below 10 nm is the combination of at least two effects. The first one is fluorescence enhancement due to MEF and the second one is quenching due to near by metallic particles.

Fluorescence lifetimes of probes contain a wealth of information related to the system being investigated revealing the microenvironments around the fluorophores. Additionally, a combination of quantum yield and lifetime can reveal the effects of the metal particles as the radiative and non-radiative decay rates of the fluorophores. To understand more about the effect of probe distance from the SIFs on the observed MEF and SIFs quenching ability on the SRB, we measured the fluorescence intensity decays for all SRB incorporated ODA layers deposited on both SIFs and glass surfaces. Figure 7 shows the corresponding fluorescence intensity decays. Interestingly, the intensity decay of the probe on SIFs with 5 nm distance show shortest decay time and the average lifetimes are consistently increased with increasing the distance from the SIFs surface from 5 to 50 nm. Furthermore the SRB layer within contacting distance (*i.e.* 0 nm) from the SIFs surface show longer decay than the SRB probes positioned at a distance of 5 nm from the SIF surface. On the other hand, within the experimental errors, the corresponding fluorescence intensity decays of the probes deposited with any distance from the glass surface show very similar lifetimes (the intensity decay of monolayer on glass is shown in Figure 4). The ratio of the average lifetimes of each particular probe layer on glass and that of on SIFs surface was plotted as a function of the distance from the SIF surface (Figure 6). The highest factor of reduction in fluorescence lifetime of about 7.5-fold is observed from the SRB incorporated ODA layers deposited on SIFs with 5 nm distance from the surface and it reduces to ~2-fold when the probes are spaced by 50 nm distance. The observed lifetime decreases on SIFs surface with any distance might be result of at least two processes. One of which is due to an increase in the radiative decay rate and the second is due to the increased non-radiative interactions of the probes with the metallic surface. Although it is difficult to draw a boarder line between the contributions from each of these two processes, we believe an increase in the radiative decay rate is the dominant reason for the decreases in lifetime shown in Figure 7. The increase in the radiative decay rate is probably largest when the probe distance from the surface is above 7–8 nm and that due to the non-radiative interactions is major below 7–8 nm from the surface.

For a heterogeneous system, steady state measurements only provide the averaged information. Time-resolved fluorescence can extract information from a heterogeneous system and could also provide the molecular population distribution of the probed system. Fluorophores positioned on metallic nano-structured substrates at varied distances is a heterogeneous system. For this reason we thought that lifetime distribution could provide a better picture of the distance-dependent metal-enhanced fluorescence. Figure 8A presents the lifetime distributions of the probe on glass. Two components one centered around 1 ns and the second one centered at ~2.5 ns were found. Note that the time-axis is different from the top panel. It is apparent from the figure that the distributions are similar for all distances of SRB molecules from the glass substrate. The lifetime distributions of SRB molecules on SIFs are shown in Figure 8B. The major lifetime distribution with a short lifetime centers around 200 ps is observed when

the SRB molecules are directly on the SIFs surface. The center of this short lifetime distribution shifts monotonically towards longer lifetimes with increasing the distance of the probe from the metalized surface and the FWHM of this Gaussian distribution is systematically increased. Combining all the lifetime distributions in a single plot (Figure 8C), it is apparent that the lifetime distributions on SIFs are significantly different than that on glass. These effects on the lifetime distributions are of particular interest because they provide insight into the range of environments experienced by the fluorophores. The distributions suggest a single average environment for the probe on glass, and a range of environments for the probe on the SIFs.

Our results demonstrate that the fluorescence intensities (quantum efficiencies) and lifetimes (radiative decay rates) varies with the distance between the probe monolayer and metal nanostructures. The increases in the rates of emission (N_r) and excitation (N_{ex}) between the metal and fluorophore can be interrelated by[15]

$$N_r(d)=N_r^{(d=0)}\exp\left(-\frac{d}{R_r}\right)+1 \tag{11}$$

$$N_{ex}(d)=N_{ex}^{(d=0)}\exp\left(-\frac{d}{R_{ex}}\right)+1 \tag{12}$$

where d is the distance between the metal and fluorophore, R_r and R_{ex} are the characteristics distances over which these effects decrease to 1/e exponentially. The total fluorescence intensity in the presence of metal (I_m) as a function of metal-fluorophore distance d is given by:

$$I_m=I_0\frac{\Phi_m}{\Phi_0}N_{ex}(d) \tag{13}$$

where I_0 is the measured intensity in the absence of metal. The ratio of fluorescence quantum yields of the probes as a function of metal-fluorophore distance (d) in presence and absence of metal particles can be rewritten as:

$$\frac{\Phi_m}{\Phi_0}=\frac{N_r(\Gamma+k_{nr})}{N_r\Gamma+k_{nr}^{/}}=\frac{N_r\tau_m}{\tau_0} \tag{14}$$

Equation 13 can be deduced as:

$$I_m=I_0\frac{\tau_m}{\tau_0}\left[N_r^{(d=0)}\exp\left(-\frac{d}{R_r}\right)+1\right]\left[N_{ex}^{(d=0)}\exp\left(-\frac{d}{R_{ex}}\right)+1\right] \tag{15}$$

We used equation 15 to analyze our measured steady-state intensities and lifetimes of SRB at various distances from the SIFs surfaces. We assumed that $k_{nr} \approx k_{nr}^{/}$. We have recovered the four free parameters $N_r^{(d=0)}$, $N_{ex}^{(d=0)}$, R_r, R_{ex} in equation 15 by fitting the steady-state and time-resolved data (shown in Figure 6) by non-linear least square analysis. We have obtained $N_r^{(d=0)} = 5$; $N_{ex}^{(d=0)} = 10$; $R_r = 25$ nm and $R_{ex} = 16$ nm. The nonradiative decay rate ($k_{nr}^{/} \sim 2 \times 10^9$ sec^{-1}) estimated from the fitting agrees well with the reported literature value.[26] Furthermore, our analysis reveals that the rate of excitation is increased by a factor of 10 and arises at a distance of 16 nm. On the other hand the increase in radiative decay rate is 5-fold and this increase continues over a distance of ~25 nm.

It is informative to show the distance dependent changes of radiative decay and excitation rates. These rates were obtained from equations 11 and 12 and the measured spectral parameters. The changes in radiative decay rate and rate of excitation as a function of distance between the fluorophore and SIFs surfaces are shown in Figure 9. These results suggest that enhanced

excitation occurs below 10 nm and the increase in radiative rate (N_r) on SIFs surface decreases with increased distances over 25 nm.

4. Summary

SRB incorporated octadecylamine LB layers deposited on silver island films are used to study the distance-dependent metal-enhanced fluorescence. Inert stearic acid layers are used to control the distance between the probe and metallic nanostructured surfaces. The maximum enhancement of fluorescence near a factor of 7 was observed with the probe distance of 10 nm from the SIFs surface and the enhancement decreases to 2-fold when the probe is separated by 50 nm. The minimum fluorescence lifetime was observed when the SRB molecules are 5 nm from the SIFs surface. We also present continuous lifetime distributions which can better represent the observed heterogeneous decay of the fluorophore on SIFs substrate. The evolution of the lifetime values as a function of the distance between the metal nanostructure and probe is studied. Lifetime distributions of SRB on SIFs at multiple distances show different central lifetime values. In this systematic steady-state and time-resolved spectroscopic study, we described the effect of probe distance from the silver nanostructures on metal-enhanced fluorescence using well-defined distance and controlled orientation of fluorophores by established LB technique. The distance dependent changes of radiative decay and excitation rates of SRB in presence of metallic nanostructures are also presented. The present study reveals how the fluorophore-metal interactions changes with the distances between metal and probe.

Acknowledgements

The present work was supported by the National Institute of Health (NIH), RR-08119 and EB-00682.

References

1. Stefani FD, Vasilev K, Bocchio N, Stoyanova N, Kreiter M. Phys Rev Lett 2005;94:023005. [PubMed: 15698172]
2. Gersten, J. Topics in Fluorescence Spectroscopy. Geddes, CD.; Lakowicz, JR., editors. 8. Springer, NY: 2005.
3. Lakowicz JR. Anal Biochem 2005;337:171. [PubMed: 15691498]
4. Kasry A, Knoll W. Appl Phys Lett 2006;89:101106.
5. Anger P, Bharadwaj P, Novotny L. Phys Rev Lett 2006;96:113002. [PubMed: 16605818]
6. Kuhn S, Hakanson U, Rogobete L, Sandoghdar V. Phys Rev Lett 2006;97:017402. [PubMed: 16907406]
7. Shimizu KT, Woo WK, Fisher BR, Eisler HJ, Bawendi MG. Phys Rev Lett 2005;95:017402. [PubMed: 16090656]
8. Cannone F, Chirico G, Bizzarri AR, Cannistraro S. J Phys Chem B 2006;110:16491. [PubMed: 16913781]
9. Barnes WL. J Mod Opt 1998;45:661.
10. Lakowicz JR. Anal Biochem 2001;298:1. [PubMed: 11673890]
11. Lakowicz JR, Shen Y, D'Auria S, Malicka J, Fang J, Grcyzynski Z, Gryczynski I. Anal Biochem 2002;301:261. [PubMed: 11814297]
12. Lakowicz JR. Plasmonics 2006;1:5.
13. Ray K, Badugu R, Lakowicz JR. J Am Chem Soc 2006;128:8998. [PubMed: 16834349]
14. Sokolov K, Chumanov G, Cotton TM. Anal Chem 1998;70:3898. [PubMed: 9751028]
15. Malicka J, Gryczynski I, Gryczynski Z, Lakowicz JR. Anal Biochem 2003;315:57. [PubMed: 12672412]
16. Tarcha PJ, DeSaja-Gonzalez J, Rodriguez-LIorente S, Aroca R. Appl Spectrosc 1999;53:43–48.

17. Antunes PA, Constantino CJL, Aroca RF, Duff J. Langmuir 2001;17:2958.
18. Ray K, Badugu R, Lakowicz JR. J Phys Chem B 2006;110:13499. [PubMed: 16821876]
19. Ray K, Badugu R, Lakowicz JR. Langmuir 2006;128:8374. [PubMed: 16981751]
20. Ulman, A. An introduction to ultrathin organic films: from Langmuir-Blodgett to self-assembly. Academic Press; San Diego: 1991.
21. Ray K, Nakahara HJ. Phys Chem B 2002;106:92.
22. Lakowicz, JR. Principles of Fluorescence Spectroscopy. 2. Kluwer Academic/Plenum Publishers; New York: 1999.
23. Yguerabide J, Yguerabide EE. Anal Biochem 1998;262:137. [PubMed: 9750128]
24. Yguerabide J, Yguerabide EE. Anal Biochem 1998;262:157. [PubMed: 9750129]
25. Schultz S, Smith DR, Mock JJ, Schultz DA. Proc Natl Acad Sci 2000;97:996–1001. [PubMed: 10655473]
26. Lavallard P, Rosenbauer M, Gacoin T. Phys Rev A 1996;54:5450. [PubMed: 9914124]

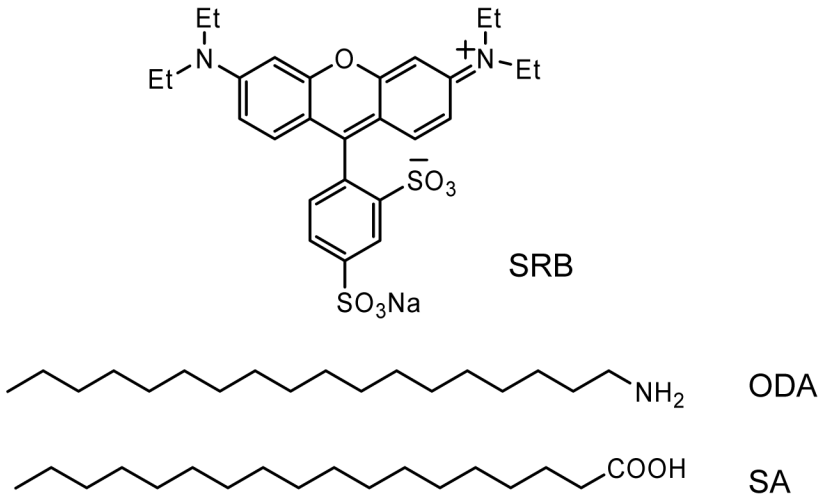

Figure 1.
Chemical structures of sulforhodamine (SRB) and the long-chain amphiphilic molecules stearic acid (SA) and octadecylamine (ODA) used for LB deposition.

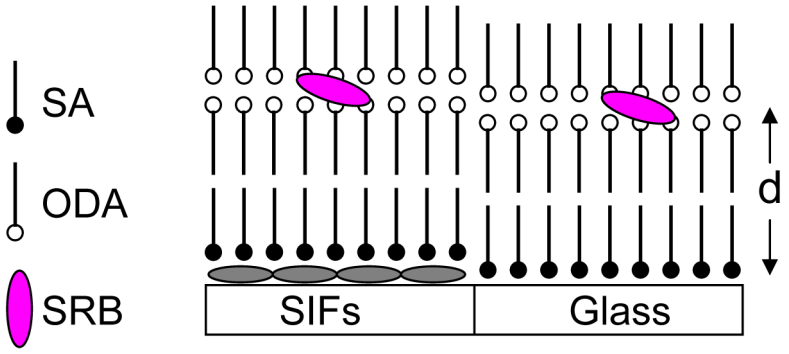

Figure 2.
Schematic representation of Langmuir-Blodgett layers construction and subsequent electrostatically adsorbed SRB dye molecules at ODA layers. ODA layers were spaced by inert SA layers from the substrate. d is the distance between fluorophore and SIF surface that can be varied with the numbers of inert SA layers at a resolution of ~ 2.5 nm.

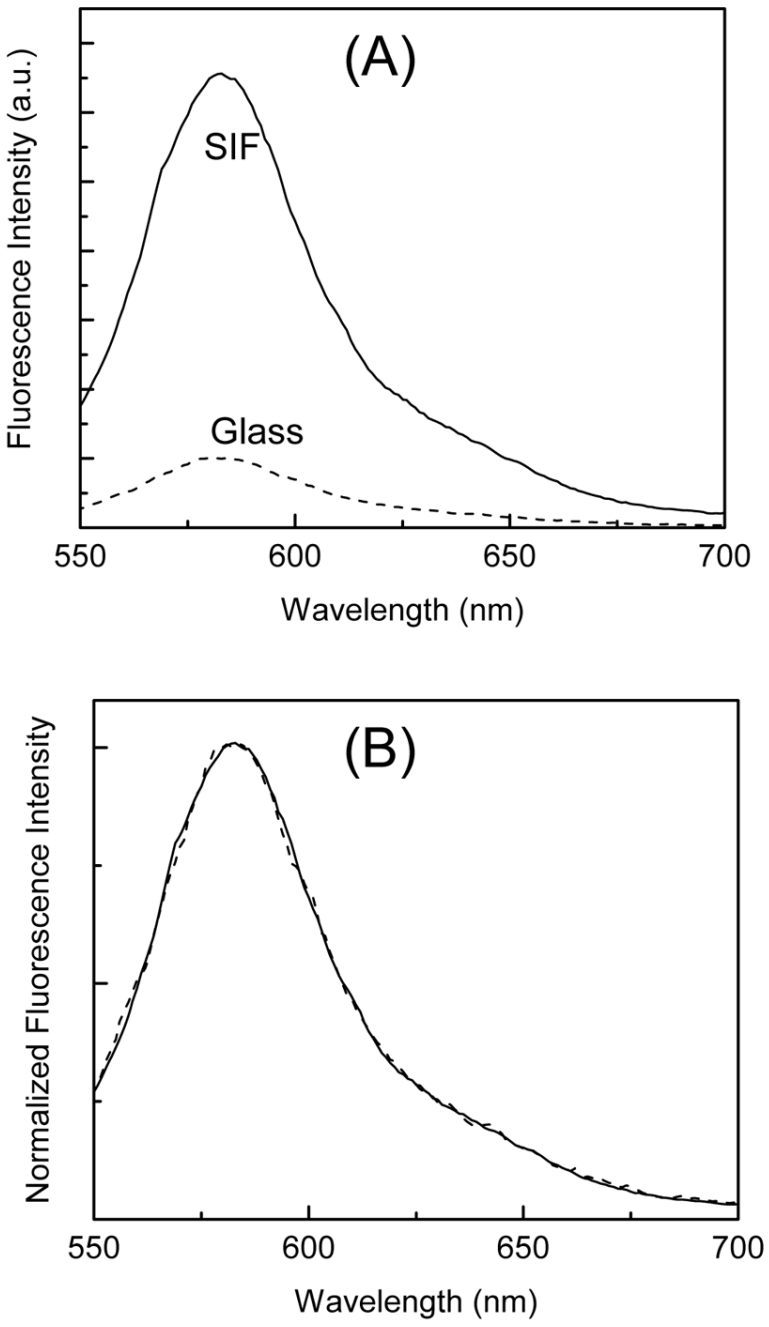

Figure 3.
(A) Emission spectra of SRB incorporated into LB layers deposited on glass and SIFs surfaces and the panel B shows the corresponding intensity normalized emission spectra.

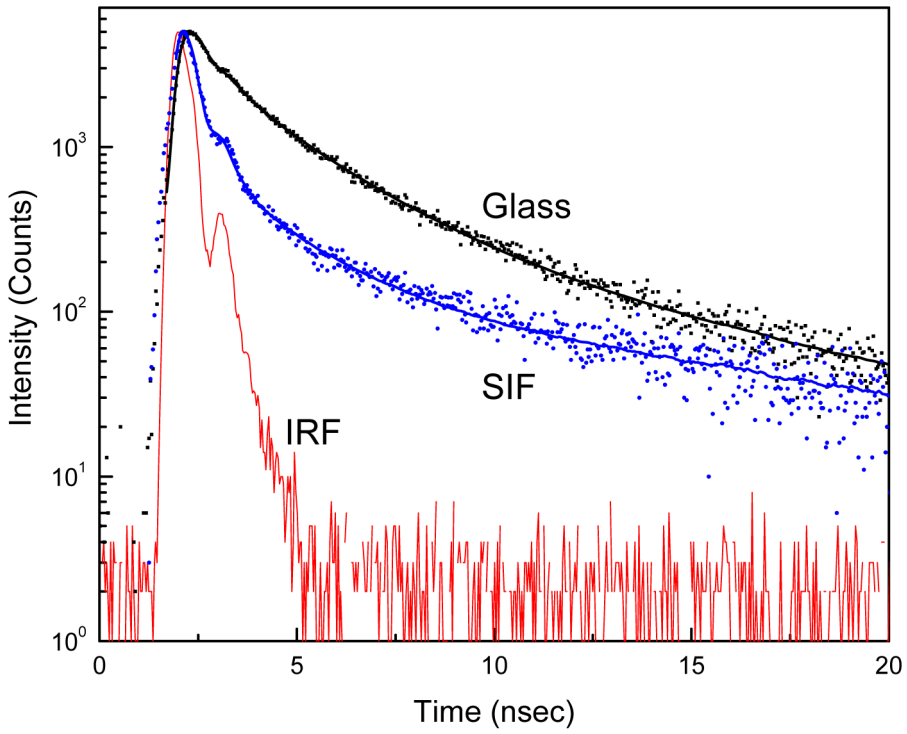

Figure 4.
Fluorescence intensity decays of SRB incorporated in ODA layers on glass and SIFs. Instrument response function (IRF) is also included.

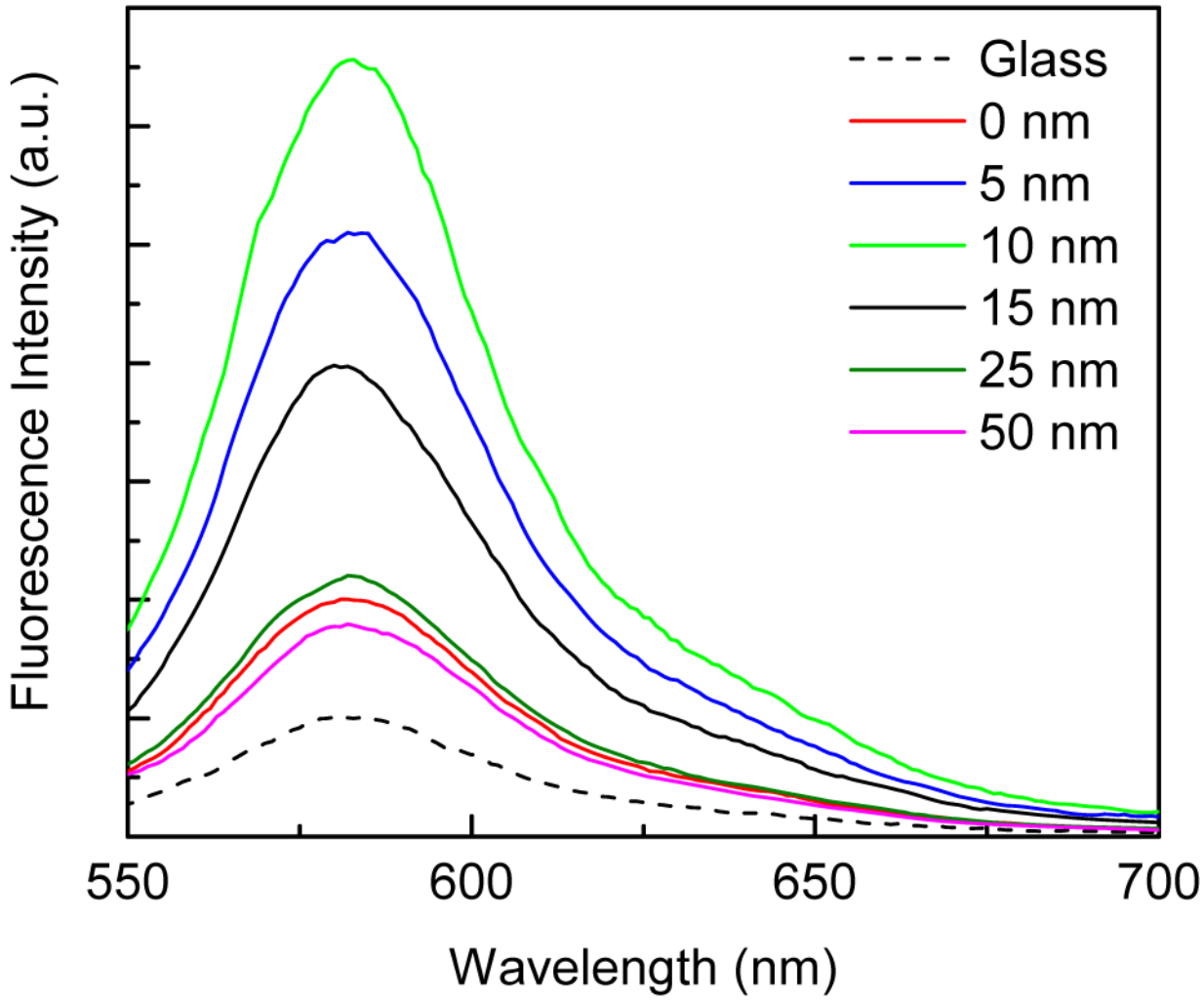

Figure 5.
Emission spectra of SRB incorporated ODA layers deposited at various distances from SIFs surface. Fluorescence spectrum of SRB on glass surface is also included (dash line).

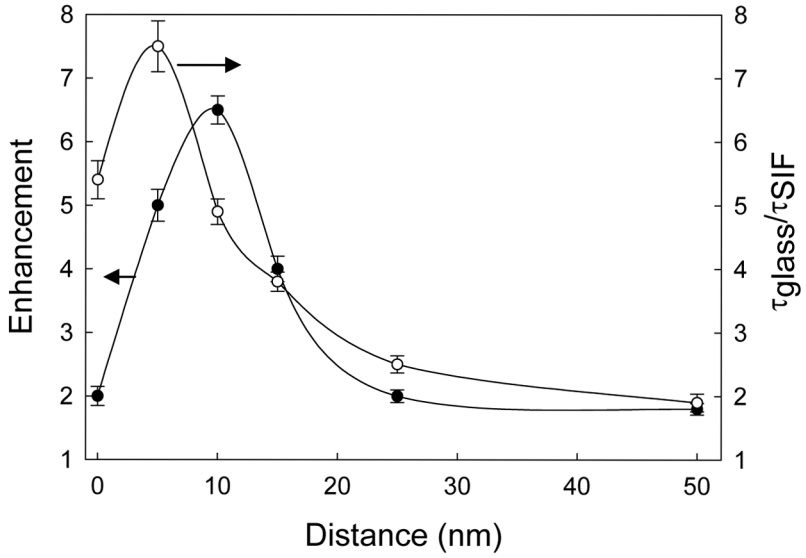

Figure 6.

Fluorescence intensity decays of SRB on SIFs surface at various distances. The dots and the lines represent the data and multi-exponential fits respectively. The lower solid line is the impulse response function (IRF) for the instrument.

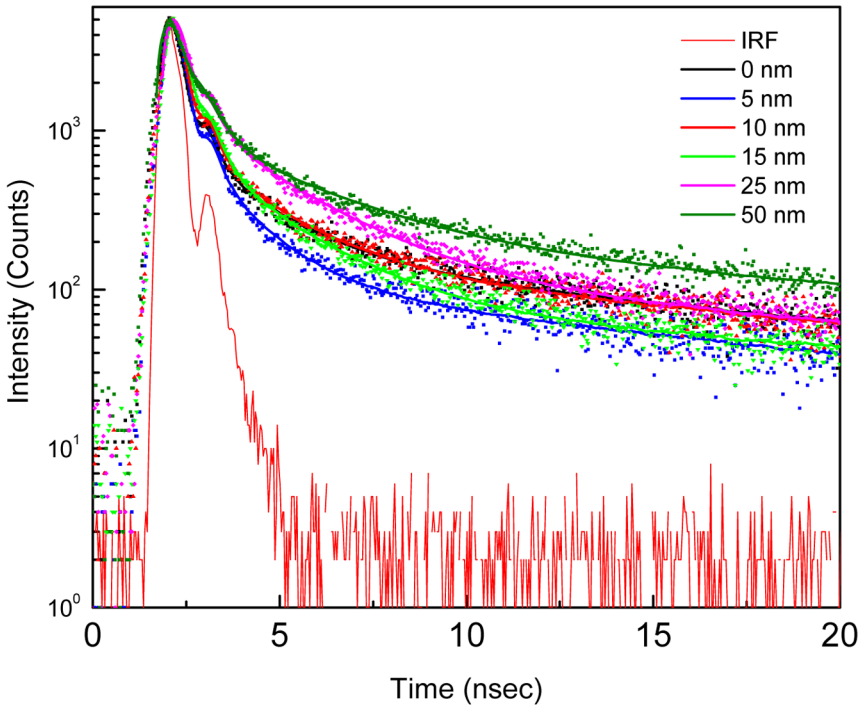

Figure 7.
Fluorescence enhancement factor and corresponding ratio of lifetimes of SRB on glass and SIFs surfaces versus distance from the SIFs surface.

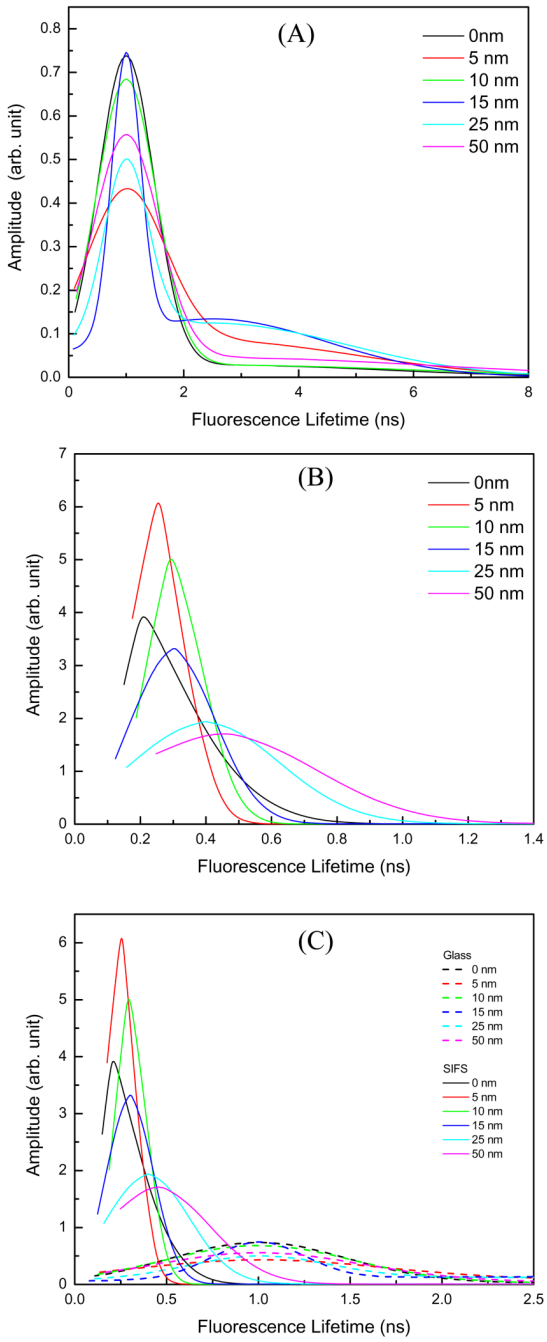

Figure 8.
Fluorescence lifetime distributions of SRB at varied distances from (A) Glass and (B) SIFs substrates. (C) Combining the lifetime distributions of (A) & (B).

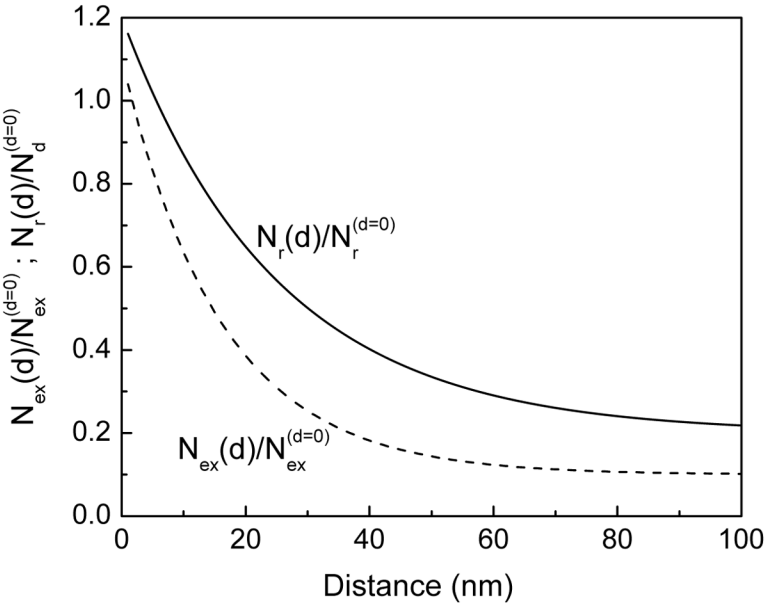

Figure 9.
Normalized rate of excitation [$N_{ex}(d)/N_{ex}^{(d=0)}$] and rate of radiative decay [$N_r(d)/N_r^{(d=0)}$] as a function of SRB distance from the SIF surface.